

# Sensitivity and Non-linearity Study and Performance Enhancement in Bossed Diaphragm Piezoresistive Pressure Sensor

Ramprasad Nambisan

Department of Electrical & Electronics Engineering  
Birla Institute of Technology and Science (BITS)  
Pilani, Rajasthan, India

S. Santosh Kumar, and B. D. Pant

MEMS and Microsensors Group  
CSIR-Central Electronics Engineering Research Institute  
(CEERI)  
Pilani, Rajasthan, India  
E-mail: santoshkumar.ceeri@gmail.com

**Abstract**—This paper describes a comparative study of sensitivity and non-linearity of conventional and bossed diaphragm piezoresistive pressure sensor along with a performance enhanced design. The proposed structures take into consideration corner compensation to avoid distortion of the mesa structure during fabrication of bossed diaphragm structure using wet bulk micromachining. Optimum piezoresistors locations are calculated with the help of simulations carried out using finite element method (FEM) based tool COMSOL® Multiphysics. Since the sensitivity and non-linearity of conventional and bossed diaphragm structures showed a linear trend, empirical formulae are proposed using linear fit for quick and approximate calculation of sensitivity and non-linearity for a particular sensor structure. It is observed that high stress regions are also present near the boss – diaphragm interface and hence a design with piezoresistors placed at these regions is also proposed. This design is found to be enhancing the performance of piezoresistive pressure sensor compared to the conventional piezoresistor placement.

**Keywords**— Piezoresistive pressure sensor; MEMS; FEM

## I. INTRODUCTION

MEMS pressure sensors are widely used in applications ranging from attitude sensing, tire-pressure sensing to biomedical applications like intraocular pressure sensing, intracranial pressure sensing etc. [1]. The prominent transduction mechanisms used in sensing pressure are capacitive, piezoresistive, resonant and piezoelectric. Among these, piezoresistive pressure sensors are popular because of high reliability, high linearity, easy compensation circuit and ease of fabrication [2].

A conventional piezoresistive pressure sensor consists of an etched silicon diaphragm bonded over a pyrex glass as shown in Fig. 1. As pressure is applied, the diaphragm is deflected and stress regions are formed. The piezoresistors placed at these regions in turn experience stress and their resistance changes. This change in resistance results in change in output voltage corresponding to the pressure applied.

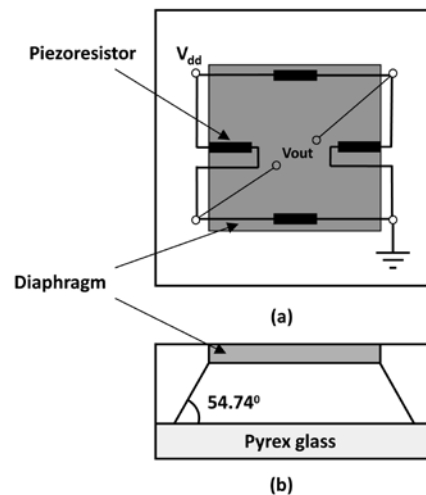


Fig. 1. Schematic of a typical pressure sensor. (a) Top view. (b) Cross-sectional view.

For a particular pressure range, the conventional structure can be optimized to achieve high performance by optimizing the position of piezoresistors over the diaphragm, diaphragm dimension, and diaphragm thickness. However, at low pressure ranges, the diaphragm size must be increased and thickness reduced to get acceptable sensitivity. This results in an increase in the non-linearity of output of pressure sensor. One corrective measure to this problem is to locally stiffen the diaphragm, thereby limiting the deflection [3]. This was achieved by Stedman [4]. He employed a round boss on a round diaphragm and later Pien employed a double boss structure [5]. This local stiffening results in reduction of deflection of diaphragm and thus the non-linearity is improved. Although bossed structures have been previously proposed, there is no exhaustive study which assays the effect of implementation of boss as well as effect of boss size. In this paper, we present a thorough analysis of bossed design pressure sensor and its comparison with conventional design. The performance of bossed design is further enhanced by placing the piezoresistor at the regions near boss-diaphragm interface instead of conventional placement. Conventional diaphragm structure and bossed mesa structure obtained using wet bulk micromachining are assumed.

## II. THEORY

In piezoresistive pressure sensors, silicon is preferred as the material for diaphragm owing to desirable characteristics like excellent mechanical properties and reproducible elastic deformations [6]. Using analytical equations for analysis can lead to limiting the accuracy because of difference in clamping conditions of a plate and an actual diaphragm [7]. Also, it is difficult to obtain the analytical solutions in case of complex structures like bossed diaphragms. Therefore, in this work FEM tool COMSOL<sup>®</sup> is used for the electromechanical analysis of the pressure sensor. For accuracy, anisotropic material properties of silicon are considered in the present work [8]. The basic theory of piezoresistance is well known and was proposed by Smith in 1954 [9].

The change in resistance of a piezoresistive material under stress is given by [10]:

$$\frac{\Delta R}{R} = \frac{\Delta l}{l} - \frac{2\Delta r}{r} + \frac{\Delta \rho}{\rho} \quad (1)$$

where  $\Delta R, \Delta l, \Delta r, \Delta \rho$  are changes in resistance, length, width and resistivity, respectively.  $R, l, r, \rho$  are the initial resistance, length, width and resistivity, respectively. Since the first two terms corresponds to geometrical deformation and are negligible in the case of semiconductors/piezoresistors, the equation reduces to [10]:

$$\frac{\Delta R}{R} = \frac{\Delta \rho}{\rho} = \pi_l \sigma_l + \pi_t \sigma_t \quad (2)$$

where  $\pi_l, \pi_t$  correspond to piezoresistive coefficients of the material along longitudinal and transverse directions, respectively.  $\sigma_l, \sigma_t$  are the corresponding stresses along longitudinal and transverse directions, respectively. In the present design, p-type piezoresistor oriented along [110] directions in (100) wafers are considered to maximize the piezoresistive effect. In such a scenario, we have [9]:

$$\pi_{l,110} = \frac{1}{2}(\pi_{11} + \pi_{12} + \pi_{44}) \quad (3)$$

$$\pi_{t,110} = \frac{1}{2}(\pi_{11} + \pi_{12} - \pi_{44}) \quad (4)$$

For silicon,  $\pi_{11} = 6.6 \times 10^{-11} \text{ Pa}^{-1}$ ,  $\pi_{12} = -1.1 \times 10^{-11} \text{ Pa}^{-1}$  and  $\pi_{44} = 1.381 \times 10^{-11} \text{ Pa}^{-1}$ .

## III. CORNER COMPENSATION FOR REALIZING BOSSED DIAPHRAGM - TECHNOLOGY ASPECTS

The diaphragm of a conventional pressure sensor can be fabricated using a dry process like deep-reactive-ion-etching (DRIE) or using wet anisotropic etchants like tetramethylammonium hydroxide (TMAH). The fabrication process involving wet etching using TMAH is low cost and simple, hence it is chosen for the proposed study. However, wet etchants have different etching rates for different crystallographic planes of silicon.

For a bossed diaphragm, the expected shape after realization of the diaphragm structure is shown by the cross-sectional view in Fig. 2 (a). Using a masking scheme as shown in Fig. 2 (b) for realizing the diaphragm using wet anisotropic etchant (like TMAH) will result in convex undercutting of the

boss. Convex undercutting is due to presence of fast etching planes of silicon such as {311} and {411}, which etches faster than other planes [11]. Due to convex undercutting, a distorted structure will be formed as shown in Fig. 2 (c) [12]. The expected mesa structure bottom view after etching is shown in Fig 2 (d). To avoid convex undercutting, corner compensation techniques are used. These corner compensation structures are included at the corners of the mask patterns in order to achieve mesa structure [13]. Fig. 3 shows some of the commonly used (or proposed) corner compensation structures.

Based on the experiments carried out for 25% wt. TMAH, the values of  $W_{sq}$ ,  $W_{ob1}$  and  $W_{ob2}$  are given by empirical formulae in Eq. (5) to (7) [11]:

$$W_{sq} = W_s + 0.58 \frac{R(311)}{R(110)} D_e \quad (5)$$

$$W_{ob1} = W_s + 1.414 \frac{R(311)}{R(110)} D_e \quad (6)$$

$$W_{ob2} = W_s + \left[ 0.351 + 0.734 \frac{R(311)}{R(110)} \right] D_e \quad (7)$$

where  $\frac{R(311)}{R(110)}$  is anisotropic etch ratio equal to 2.23,  $W_s$  is minimal spacing and  $D_e$  is etch depth. In this study, the minimal spacing is chosen to be  $10 \mu\text{m}$ . The etch depth will be dependent upon the desired substrate and diaphragm thickness. The square compensation is chosen for the study as for the same diaphragm size, it minimizes the area for the corner compensation structure, thereby maximizing the boss size compared to other two compensation schemes.

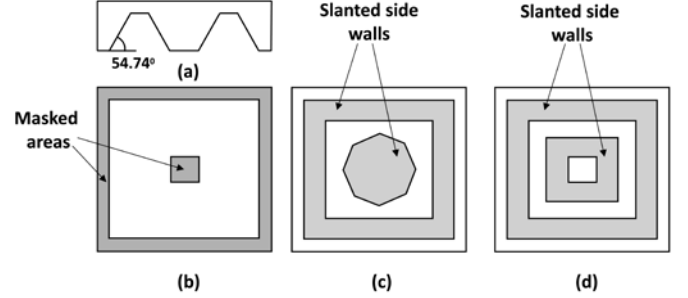


Fig. 2. (a) Cross-sectional view of expected structure. (b) Schematic of mask without corner compensation structure. (c) Bottom view of distorted structure formed due to undercutting. (d) Bottom view of expected bossed diaphragm structure

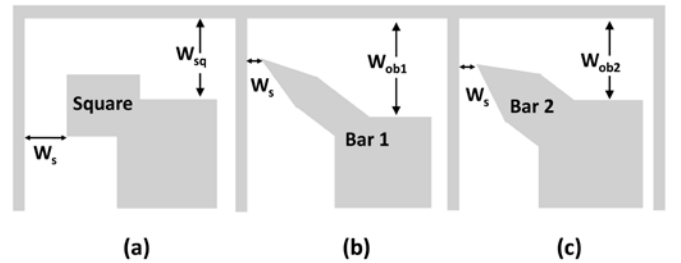


Fig. 3. Commonly used corner compensation structures

## IV. DESIGN PARAMETERS AND METHODOLOGY

For the design study of bossed diaphragm pressure sensors, a typical chip size of  $4 \text{ mm} \times 4 \text{ mm}$  is chosen. The substrate is

n-type (100) silicon with p-type piezoresistors placed along <110> direction for maximizing sensitivity [14]. Bossed diaphragm pressure sensors are especially useful for low pressure applications and therefore in this work a pressure range of 0-1.1 bar is chosen. A bias voltage of 5V is used for all the simulated designs. This pressure range is useful for barometric applications. Keeping in view the low pressure range and ease of fabrication, a diaphragm of 20  $\mu\text{m}$  thickness is used. A square diaphragm is used for the study and the diaphragm edge length is varied from 1400  $\mu\text{m}$  to 2000  $\mu\text{m}$  in step of 100  $\mu\text{m}$ . The substrate thickness is chosen as 350  $\mu\text{m}$  as the optimized sensor design would be fabricated on a 3 inch wafer. To compare the performance of bossed diaphragm pressure sensor and a conventional pressure sensor, first a conventional pressure sensor with the above specification is analyzed. The cross-section of the schematic of the conventional sensor structure is shown in Fig. 4.

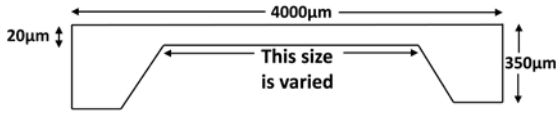


Fig. 4. Cross-section of diaphragm structure for a conventional pressure sensor

Rectangular piezoresistors with a dimension of 120  $\mu\text{m} \times 10 \mu\text{m}$  are used for the study. The positions of piezoresistors are optimized as follows. The change in resistance of piezoresistors is related to the stress experienced by the piezoresistor and is given by Eq. (2). If the x- and y-directed stresses experienced by the piezoresistors is given by  $\sigma_x$  and  $\sigma_y$ , then the change in resistance of the piezoresistors can be given by:

$$\frac{\Delta R}{R} = \pi_l \sigma_x + \pi_t \sigma_y \quad (8)$$

The x- and y-directed stress at the points (on the sensor structure) along two cutlines, cutline-1 (along x-axis) and cutline-2 (along y-axis) are determined. The cutlines are shown in Fig. 5.

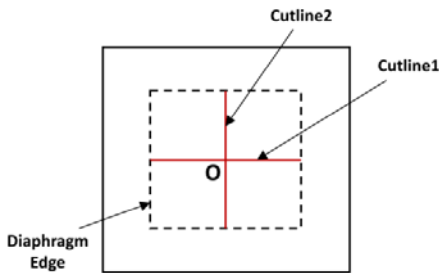


Fig. 5. Cutlines used for determining high stress regions

For the two piezoresistors placed symmetrically around the center of the diaphragm on cutline-1, Eq. (8) can be used to determine the  $\Delta R/R$  along cutline-1. This plot will be used for optimizing the position of longitudinal piezoresistors. The  $\Delta R/R$  for these piezoresistors must be maximized for maximizing sensitivity and therefore the center of these two piezoresistors are placed at the two points where  $\Delta R/R$  is maximized. For the two piezoresistors placed symmetrically around the center of the diaphragm on cutline-2, again Eq. (8) can be used to determine the  $\Delta R/R$  along cutline-2. This plot

will be used for optimizing the position of transverse piezoresistors. As the piezoresistors are connected in Wheatstone bridge, the  $\Delta R/R$  for these piezoresistors must be minimized for maximizing sensitivity and therefore, the center of these two piezoresistors are placed at the two points where  $\Delta R/R$  is minimized. For design simulations using COMSOL<sup>®</sup>, Aluminium is used as conductor for connecting the piezoresistors in Wheatstone bridge configuration. The designed structures are meshed “extremely fine” with tetrahedral elements. The pressure is applied from 0 bar to 1.1 bar with an interval of 0.1 bar. These simulation parameters are consistently used throughout the study.

## V. CONVENTIONAL DIAPHRAGM PRESSURE SENSOR WITH CONVENTIONAL PIEZORESISTOR CONFIGURATION

The conventional structure (without boss) for pressure sensor along with piezoresistors and conductors is designed in COMSOL and as a representative example, the value of  $\Delta R/R$  along cutline-1 and cutline-2 for a diaphragm size of 1700  $\mu\text{m} \times 1700 \mu\text{m}$  is shown in Fig. 6.

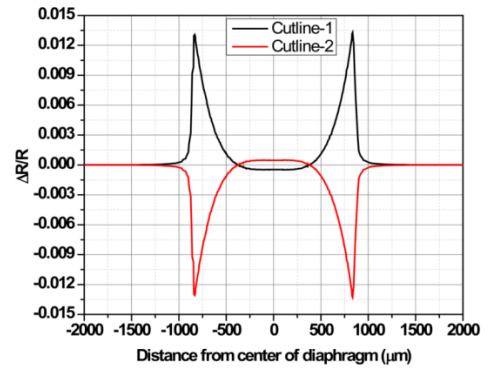


Fig 6.  $\Delta R/R$  along cutline-1 and cutline-2 for a diaphragm size of 1700  $\mu\text{m} \times 1700 \mu\text{m}$

The x-axis of Fig. 6 indicates the distance from the center along cutline-1 and cutline-2. As can be observed from the figure, the maxima for cutline-1 and minima for cutline-2 are both observed close to the edge of the diaphragm. The piezoresistors are placed with their center at these points. Similarly, for all the other square diaphragms with edge length from 1400  $\mu\text{m}$  to 2000  $\mu\text{m}$ , the optimized piezoresistor locations are similarly obtained.

## VI. SIMULATION RESULTS FOR CONVENTIONAL DIAPHRAGM PRESSURE SENSOR WITH CONVENTIONAL PIEZORESISTOR CONFIGURATION

There are several performance parameters for a piezoresistive pressure sensor such as sensitivity, non-linearity, hysteresis, repeatability and the effect of temperature on span and offset. However, at the design phase, sensitivity and non-linearity of the sensor are the most important parameters for optimization [10]. For each sensor structure with diaphragm edge length from 1400  $\mu\text{m}$  to 2000  $\mu\text{m}$ , the optimized piezoresistor locations are determined as indicated in the previous section. The piezoresistors are placed at these optimized locations for different sensor structures and the sensitivity and non-linearity is determined in each case. The sensitivity vs. diaphragm edge length is plotted in Fig. 7.

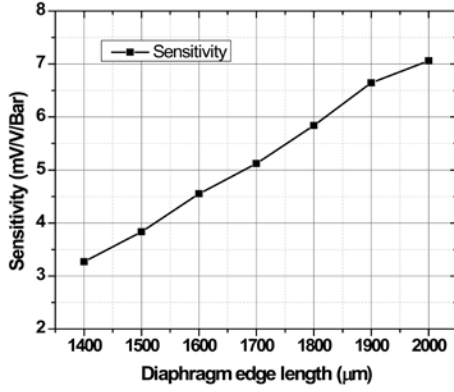


Fig. 7. Sensitivity vs. diaphragm edge length plot for conventional diaphragm pressure sensor with conventional piezoresistor configuration

It is observed that the plot shown in Fig. 7 shows approximately a linear trend. Hence, by doing a linear fit, an empirical formula is proposed for finding sensitivity as expressed by Eq. (9).

$$S = -5.917 + D \times 0.0065 \quad (9)$$

where  $S$  is sensitivity in mV/V/Bar and  $D$  is the diaphragm edge length in  $\mu\text{m}$ . Similarly, the non-linearity vs. diaphragm edge length is plotted in Fig. 8.

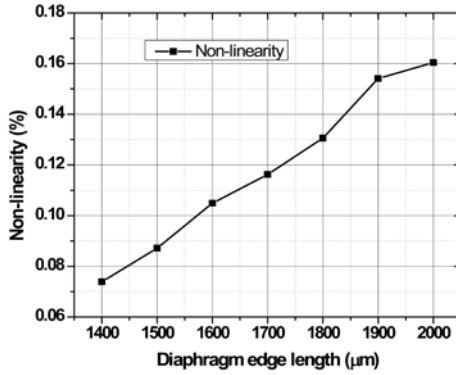


Fig. 8. Non-linearity vs. diaphragm edge length plot for conventional diaphragm pressure sensor with conventional piezoresistor configuration

In this case too, because of a linear trend, using linear fit, following empirical formula is proposed:

$$NL = -0.136 + D \times 1.497 \times 10^{-4} \quad (10)$$

where  $NL$  is non-linearity in %/full scale and  $D$  is diaphragm edge length in  $\mu\text{m}$ . It is observed that as diaphragm size increases, sensitivity improves but non-linearity deteriorates, which is quite natural.

## VII. BOSSSED DIAPHRAGM PRESSURE SENSOR WITH CONVENTIONAL PIEZORESISTOR CONFIGURATION

For the bossed diaphragm sensor structure, the same physical parameters and design principles are followed as discussed earlier. The schematic of the cross-section of bossed diaphragm sensor structure is shown in Fig. 9. The boss has a square shaped base. The boss size is defined as the length of base of the boss as shown in Fig. 9. As described earlier in the

paper, a square compensation is used and using Eq. (5) the maximum possible boss size for each diaphragm size is calculated and analysis is carried for each of the diaphragm size. The boss size for each diaphragm dimension is varied from 100  $\mu\text{m}$  up to the maximum allowed value for that diaphragm size.

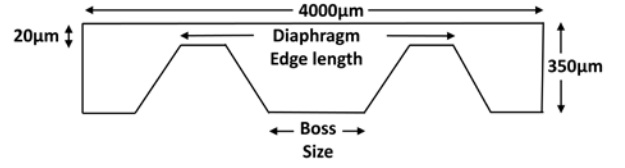


Fig. 9. Cross-section of bossed diaphragm sensor structure

As a representative example, the value of  $\Delta R/R$  along cutline-1 and cutline-2 for a diaphragm size of 1700  $\mu\text{m} \times 1700 \mu\text{m}$  with boss size of 400  $\mu\text{m}$  is shown in Fig. 10.

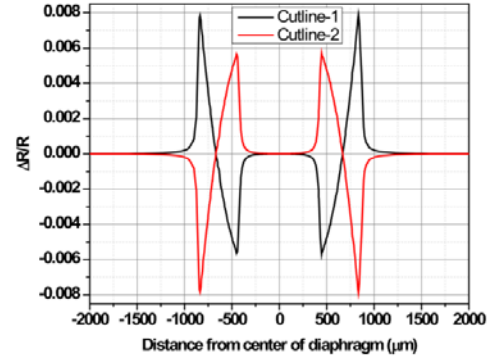


Fig. 10.  $\Delta R/R$  along cutline-1 and cutline-2 for a diaphragm size of 1700  $\mu\text{m} \times 1700 \mu\text{m}$  with boss size of 400  $\mu\text{m}$

Again, the distance from the center along cutline-1 and cutline-2 is represented by the x-axis in Fig. 10. However, unlike the conventional diaphragm case as shown in Fig. 6, here there are two maxima and two minima for both cutline-1 and cutline-2. This is due to the presence of the central boss. Again, the maxima for cutline-1 and minima for cutline-2 are both observed near the edge of the diaphragm. The piezoresistors are placed with their center at these points with placement similar to that in a conventional diaphragm pressure sensor. Similarly, for all the other square diaphragms with edge length from 1400  $\mu\text{m}$  to 2000  $\mu\text{m}$  and boss size from 100  $\mu\text{m}$  up to the maximum allowed value, the optimized piezoresistors locations are similarly obtained.

## VIII. SIMULATION RESULTS FOR BOSSSED DIAPHRAGM PRESSURE SENSOR WITH CONVENTIONAL PIEZORESISTOR CONFIGURATION

After All the structures (as mentioned in the previous section) are simulated, and the sensitivity and non-linearity are calculated. The combined plot of sensitivity vs. boss size and non-linearity vs. boss size for different diaphragm edge lengths are plotted in Fig. 11 and Fig 12, respectively.

It is observed that for a particular diaphragm size, as the boss size increases the non-linearity improves but the sensitivity deteriorates. Since both these plots show approximately a linear trend, using linear fit, the following empirical formulae are derived for sensitivity and non-linearity for a given diaphragm size and boss size:

$$S = (-6.784 + D \times 0.671 \times 10^{-2}) + B \times (-0.016 - D \times 2.393 \times 10^{-4}) \quad (11)$$

$$NL = (-0.153 + D \times 1.526 \times 10^{-4}) + B \times (0.037 - D \times 5.427 \times 10^{-4}) \quad (12)$$

where  $S$  is sensitivity in mV/V/Bar,  $NL$  is non-linearity in %/full scale,  $D$  is diaphragm edge length in  $\mu\text{m}$  and  $B$  is boss size in  $\mu\text{m}$ . These expressions offer a convenient way of calculating the approximate sensitivity and non-linearity for saving time during design optimization to achieve a desired specification.

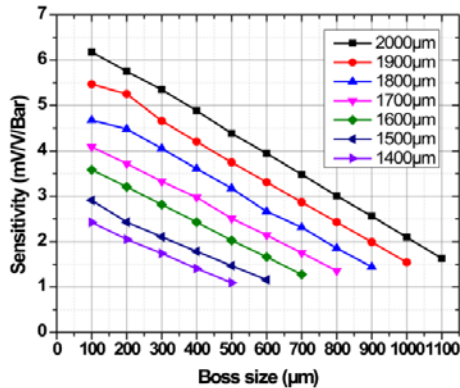


Fig. 11. Combined plot of sensitivity vs. boss size for different diaphragm edge lengths

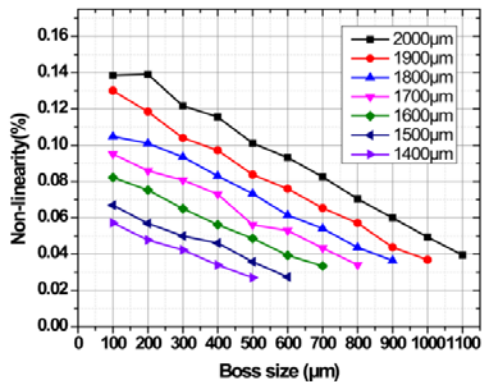


Fig. 12. Combined plot of non-linearity vs. boss size for different diaphragm edge lengths

#### IX. BOSSSED DIAPHRAGM PRESSURE SENSOR WITH STRAIGHT PIEZORESISTOR CONFIGURATION FOR PERFORMANCE ENHANCEMENT

All From Fig. 10, it can be observed that the maxima/minima for change in resistance ( $\Delta R/R$ ) for the bossed structures are also formed near the regions where the boss is attached to the diaphragm. Therefore, these high stress regions can also be used to place the piezoresistors to harness the stress in these regions. In order to achieve this goal, a different type of piezoresistor configuration is suggested as shown in Fig. 13. This piezoresistor configuration is referred to as straight piezoresistor configuration in this paper. In this piezoresistor arrangement, the outer two piezoresistors are placed with their center at the maxima of  $\Delta R/R$  near the diaphragm edge. The inner two piezoresistors are placed near the region where the boss meets the diaphragm with their center at the minima of

$\Delta R/R$ , formed at these regions. The advantage of this arrangement is that although the minima in this case are lower than the minima experienced by the transverse piezoresistors (in conventional configuration), the piezoresistors lie over a larger region of high stress region because of being present length wise over the minima. This helps in increasing the sensitivity of the sensor. Also, this design is more insensitive to misalignments. When a conventional piezoresistor configuration is used, a slight misalignment of transverse piezoresistors can lead to a significant decrease in stress experienced by it as it is present breadth wise on the minima. However, in the configuration shown in Fig. 13, there will be lesser change because it is arranged length wise on the high stress regions.

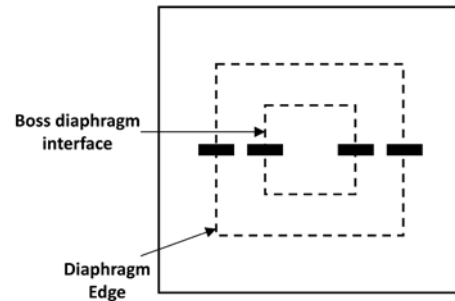


Fig. 13. Bossed diaphragm pressure sensor with straight piezoresistor configuration for performance enhancement

In order to prove the performance enhancement using the bossed diaphragm structure with configuration as shown in Fig. 13, simulations are performed for all the diaphragm sizes from  $1400 \mu\text{m}$  to  $2000 \mu\text{m}$  keeping the boss size is fixed at  $400 \mu\text{m}$ . The results obtained by these simulations are compared with the results obtained for the conventional and bossed diaphragm pressure sensor with conventional piezoresistor configuration in the next section.

#### X. CONSOLIDATED RESULTS AND COMPARISON

Simulation results (sensitivity and non-linearity) are obtained by using the straight piezoresistor configuration for the  $400 \mu\text{m}$  boss with different diaphragm sizes. The nomenclature used in the comparative study to describe the different designs discussed in the paper is listed in Table I.

TABLE I. NOMENCLATURE FOR DIFFERENT DESIGNS DISCUSSED IN THE PAPER

Design	Short name (Nomenclature)
Conventional diaphragm pressure sensor with conventional piezoresistor configuration	Conventional
Bossed diaphragm pressure sensor with conventional piezoresistor configuration	Design 1
Bossed diaphragm pressure sensor with straight piezoresistor configuration	Design 2

The sensitivity and non-linearity of Conventional, Design 1 and Design 2 for different diaphragm sizes are plotted in

Fig. 14 and Fig. 15, respectively. For Design 1 and Design 2, the results are shown for a boss size of 400  $\mu\text{m}$ .

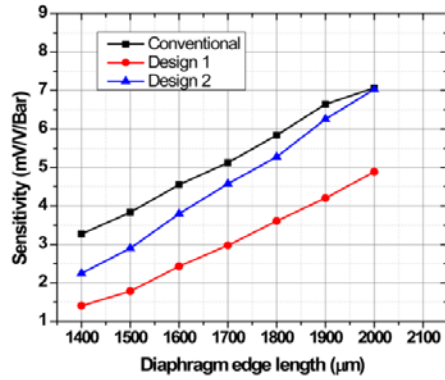


Fig. 14. Comparison of sensitivities of different designs for different diaphragm edge lengths

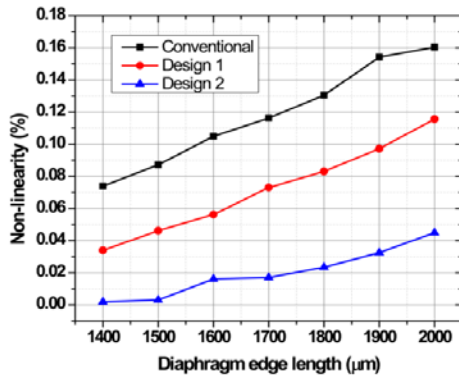


Fig. 15. Comparison of non-linearity of different designs for different diaphragm edge lengths

It can be inferred from Fig. 14 that there is a decrease in sensitivity (for all diaphragm sizes) for Design 1 compared to the conventional design. This is due to the presence of a boss structure which increases the rigidity of diaphragm just as increasing the diaphragm thickness decreases the sensitivity. However, compared to Design 1, Design 2 offers a better sensitivity for all diaphragm sizes. The purpose of using bossed diaphragm is to reduce the non-linearity and the advantage of using a bossed diaphragm design (Design 1) can be seen in Fig. 15. For all the diaphragm sizes, Design 1 gives a lower non-linearity than the conventional design. But again in comparison to Design 1, Design 2 (with straight piezoresistor configuration) offers a lower non-linearity. Thus, it is concluded that Design 2 shows an enhanced performance compared to Design 1 for both the design parameters (higher sensitivity and non-linearity).

## XI. DISCUSSIONS AND CONCLUSION

This paper first discusses the design of a conventional piezoresistive pressure sensor. Using linear fit, the trends of sensitivity and non-linearity for different diaphragm dimension are expressed in the form of simple expressions. Further, a comprehensive study on the design of bossed diaphragm pressure sensor design is carried out. For bossed diaphragm with conventional piezoresistor arrangement, a linear trend is

observed in sensitivity and non-linearity as the boss size increases. Using linear fit, formulae are proposed in each case for sensitivity and non-linearity of the sensor for different diaphragm and boss sizes. Using these formulae, one can obtain a quick rough estimate of sensitivity and non-linearity, saving design time. For the bossed diaphragm pressure sensor, a straight piezoresistors pattern has been proposed. It is observed that highly stressed regions also develop near boss; hence two piezoresistors are placed near the region where the boss meets the diaphragm. It is found that this design leads to an increase in sensitivity along with decreased non-linearity, thereby enhancing the performance of pressure sensor. Checking the validity of these observations for different boss sizes and the effect of piezoresistor size can be the subject matter of future investigations.

## REFERENCES

- [1] A. L. Herrera-May, B. S. Soto-Cruz, F. López-Huerta, and L. A. Aguilera Cortés, "Electromechanical analysis of a piezoresistive pressure micro-sensor for low-pressure biomedical applications," *Revista Mexicana De Física*, vol. 55, pp. 14-24, 2009.
- [2] Y.-H. Zhang, C. Yang, Z.-H. Zhang, H.-W. Lin, L.-T. Liu, and T.-L. Ren, "A novel pressure microsensor with 30- $\mu\text{m}$ -thick diaphragm and meander-shaped piezoresistors partially distributed on high-stress bulk silicon region," *IEEE Sensors J.*, vol. 7, no. 12, pp. 1742-1748, Dec. 2007.
- [3] A. Yasukawa, M. Shimazoe, and Y. Matsuoka "Simulation of circular silicon pressure sensors with a center boss for very low pressure measurement," *IEEE Trans. Electron Devices*, vol. 36, pp.1295-1302, 1989.
- [4] C. K. Stedman, "Transducers with substantially linear response characteristics," U. S. Patent 3341794 A, 1967.
- [5] H. S. Pien, "Strain gage pressure transducer," U. S. Patent 3520191 A, 1967.
- [6] S. S. Kumar and B. D. Pant, "Design principles and considerations for the 'ideal' silicon piezoresistive pressure sensor: a focused review," *Microsyst. Technol.*, vol. 20, pp. 1213-1247, 2014.
- [7] S. S. Kumar and B. D. Pant, "Polysilicon thin film piezoresistive pressure microsensor: design, fabrication and characterization," *Microsyst. Technol.*, 2014. DOI: 10.1007/s00542-014-2318-1.
- [8] M. A. Hopcroft, W. D. Nix, and T. W. Kenny, "What is the Young's Modulus of Silicon?," *J. Microelectromech. Syst.*, vol. 19, pp. 229-238, 2010.
- [9] C. S. Smith, "Piezoresistance effect in germanium and silicon," *Phys. Rev.*, vol. 94, pp. 42-49, 1954.
- [10] M. Bao, *Analysis and Design Principles of MEMS Devices*. Amsterdam, The Netherlands: Elsevier, Jun. 10, 2005, pp. 247-303.
- [11] R. Mukhiya, A. Bagolini, T. K. Bhattacharyya, L. Lorenzelli, and M. Zen, "Experimental study and analysis of corner compensation structures for CMOS compatible bulk micromachining using 25 wt% TMAH," *Microelectron. J.*, vol. 42, pp. 127-134, 2011.
- [12] H. Sandmeier, H. L. Offereins, K. Kühn, W. Lang, "Corner compensation techniques in anisotropic etching of (100)-silicon using aqueous KOH," Proc. 6th Int. Conf., Solid-State Sensors and Actuators (Transducers '91), San Francisco, 1991, pp. 456-459.
- [13] R. Mukhiya, A. Bagolini, B. Margesin, M. Zen, and S. Kal, "(100) bar corner compensation for CMOS compatible anisotropic TMAH etching," *J. Microelectromech. Microeng.*, vol. 16, pp. 2458-2462, 2006.
- [14] A. A. Barlian, W.-T. Park, J. R. Mallon Jr., A. J. Rastegar, and B. L. Pruitt, "Review: Semiconductor piezoresistance for microsystems," *Proc. IEEE*, vol. 97, no. 3, pp. 513-552, Mar. 2009.